

# MODELING OF TRAIN TRACK VIBRATIONS FOR MAINTENANCE PERSPECTIVES: APPLICATION

***Tse Spartan Azoh***

PhD Candidate, National Advanced School of Agro-Industrial Sciences,  
Ngaoundere University, Cameroon

***Wolfgang Nzie***

***Bonaventure Djeumako***

Senior Lecturer, Department of Mechanical Engineering, National Advanced  
School of Agro-Industrial Sciences, Ngaoundere University, Cameroon

***Bertin Soh Fotsing***

Associate Prof., IUT-FV, Dschang University, Cameroon

---

## **Abstract**

The change of geometries, heterogeneities, degradation of components and the increase of maintenance cost of the railway track are due to the phenomenon of vibrations, which is the main problem of structural dynamic. The aim of this work is to propose a dynamic model for the prediction of rail vibrations during starting and steady state response. The DEM (Discret Elements Method) is adopted for the modeling of the vehicle. Thus components are assumed as rigid bodies mounted on series of springs and dampers with several degrees of freedoms. The rail road is discretized and modeled using FEM (Finite Elements Method). Rail-pad is modeled as a massless series of springs - dampers connected along the total contact area in between the rail and the  $m^{th}$  sleepers. The sleepers are modeled as rigid elements connected by spring-damper. The ballast is modeled as separate vibrating mass connected by spring-damper coupled together vertically and horizontally while only the stiffness and damping effects of the subgrade is taken into account. The wheel-rail contact is modeled according to Herzian theory. Newmark time discretization and Newton Raphson iteration method have been used for models simulation in MATLAB. Displacements, velocities and accelerations of each modeled subsystem of components during starting and steady state response of the vehicle are calculated. The evolution of the wheel-rail contact load is also evaluated. Proactive maintenance actions are proposed in design.

---

**Keywords:** Train-track,vibration modeling, response and maintenance perspectives

## **Introduction**

The dynamic interaction between the train and the track system has called lots of attentions in the past decades. Since they vary in complexity due to the rapid increase of technology and several degrees of freedoms systems. The first ever existing model to determine rail deflection using an infinite EB beam with a continuous longitudinal support from a Winkler foundation was proposed by Timoshenko (Zurich, 1926). From then a lot of works such as the prediction of high-frequency vibration on a railway track operating under high speed train was presented (Sato Y. ,1977), (Graissie S.L. and al., 1982), (Knothe K.L. and al., 1993), (Mazilu T., 2007),(Collette C. and al., 2008). Experiments were carried out for the measurement of vibration sources on curve and straight section on the railroad. The dynamic model for the investigation of the rail and sleepers vibration generated due to wheel-rail irregularities and under the passage of a moving train was proposed (Jabbar A. Z. and al., 2009).While a plane frames finite element that takes in consideration the train vertical displacement due to traffic was furtherly proposed(Oliveira M. H. Z. and al., 2010). Modeling and experiment of the ballast vibration were previously studied (Zhai W.M. and al., 2004). (Huan Feng, 2011) developed and simulated a 3-D numerical model for the prediction of rail road track vibration using ABAQUS, while a model to investigate the influence of vertical section parameters such as vertical slope and curve on the characteristic of wheel-rail vibration with the use of SIMPACK was later evaluated (Yang H. and al., 2012). In other to improve previous works, a numerical modeling of train induced vibration was introduced (Ferrara R. and al., 2012). They proclaim that the heterogeneity of track properties, irregularities, corrugation and the behavior of materials are parameters that must be taken into consideration when modeling and predicting railway vehicle track vibration. Rail irregularities, wheel defects and variation stiffness due to the discrete supporting of rail are the origin of vibration induced by train. Even though the model brought in different changes in analyzing the dynamic behavior of the track, it never took in consideration the effect of the sub and supper structure components during starting and steady state response of track with respect to the train effect. And more resonance of components which creates our domain of interest is not considered and evaluated

## Modeling of Train–track structure

### The vehicle model

As a mechanical structure, the components of the vehicle, CC 2600 locomotive used in Camrail (Cameroon Railways Corporation), are assumed to be rigid bodies without elastic deformation during vibrations mounted on springs and viscous dampers  $C_i$ . It is composed of a rigid body, two bogies sets of four wheels. The model shown in fig.1 is illustrative of CC 2600 locomotive with train track and tables 1- 2 represent parameters nomenclature.

### Dynamic equation of motion

The following equations are respectively modeled along the vertical  $u_i$ -axis and around rotation  $v$ -axis through  $\theta_i$  coordinates for the subsystems considered. Dynamics fundamental principle of Newton is used for that purpose sequentially.

- **Vertical and rotational displacements for the car body**

$$M_7 \ddot{u}_7(t) + C_5(\dot{u}_7(t) - \dot{u}_5(t)) + C_6(\dot{u}_7(t) - \dot{u}_6(t)) + K_5(u_7(t) - u_5(t)) + K_6(u_7(t) - u_6(t)) = f_7(t) \quad (1)$$

$$J_7 \ddot{\theta}_7(t) + C_5(\dot{\theta}_7(t) - \dot{\theta}_5(t))L_{BG} + C_6(\dot{\theta}_7(t) - \dot{\theta}_6(t))L_{BG} + K_5(\theta_7(t) - \theta_5(t))L_{BG} + K_6(\theta_7(t) - \theta_6(t))L_{BG} = 0 \quad (2)$$

- **Vertical and rotational displacements for the bogie:**

$$M_i \ddot{u}_5(t) + C_5(\dot{u}_5(t) - \dot{u}_7(t)) - C_5 L_{BG} \dot{u}_5(t) + C_1(\dot{u}_5(t) - \dot{u}_{w1}(t)) + C_2(\dot{u}_5(t) - \dot{u}_{w2}(t)) + K_5(u_5(t) - u_7(t)) - K_5 L_{BG} u_5(t) + K_1(u_5(t) - u_{w1}(t)) + K_2(u_5(t) - u_{w2}(t)) = f_5(t) \quad (3)$$

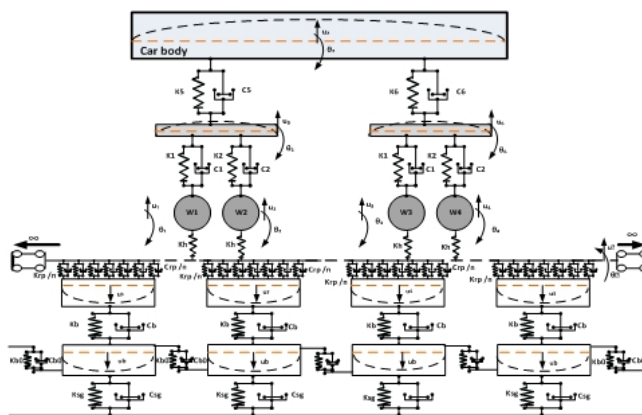


Fig.1: Locomotive CC 2600and train track Model

$$J_5 \ddot{\theta}_5 + C_1(L_w \dot{\theta}_5(t) - \dot{u}_{w1}(t))L_w + C_2(L_w \dot{\theta}_5(t) - \dot{u}_{w2}(t))L_w + K_1(L_w \theta_5(t) - u_{w1}(t))L_w + K_2(L_w \theta_5(t) - u_{w2}(t))L_w = 0 \tag{4}$$

**The wheels**

The vehicle is made up of four wheels in each bogie set that are under vertical displacement. Rotational motion involve here when the wheels are taking a curve section on the track. So for this reason, the model will be used only for straight section on the track.

$$M_{wj} \ddot{u}_{wj}(t) + C_1 ( \dot{u}_w(t) - \dot{u}_i(t) - L_w \dot{\theta}_5(t) ) + K_1(u_{w1}(t) - u_5(t) - \theta_5(t)L_w) + P_{r/w1} = f_{w1}(t) \tag{5}$$

For the (5) equation,  $L_w$ : half the distance between the center of two consecutive wheel base;  $LBG$  the distance between the center of two consecutive bogies and  $P_{r/wi}$  the wheelrail contact force  $i = (1 \div 4)$

The (5) equation after assembling can be written in the general matrix formas:

$$[M_c]\{\ddot{u}_c\} + [C_c]\{\dot{u}_c\} + [K_c]\{u_c\} - [P_{r/w}] = [F_c(t)] \tag{6}$$

$[M_c], [K_c], [C_c]$  are respectively the mass, the stiffness and damping matrices, while the  $[P_{r/w}]$  and  $[F_c(t)]$  are respectively wheel–rail interaction and load distributed one on the vehicle components.

**The wheel-rail contact model**

As a very important component of the train and track structure, the wheel-rail interaction can be formulated as a rolling contact problem

between two nonlinear profiles in the presence of friction. So in this case, the non-linear Hertzian contact theory is used to model the contact force between the  $j^{th}$  wheel and the rail. A two third power factor is used to create relationship between force and deflection (Jabbar A. Z. and al., 2009).

$$P_{w/rj}(t) = k_{hj}(u_w(t) - u_r(t) - \eta_r(t))_j^{3/2} + c_h(\dot{u}_w(t) - \dot{u}_r(t) - \dot{\eta}_r(t))_j \quad (7)$$

$$\text{If } P_{w/rj}(t) = 0 \Leftrightarrow u_{wj} \leq (u_r(t) + \eta_r(t))_j$$

For simplicity and the use of time step integration for resolving the interaction wheel and rail equation (7), the non-linear Hertzian contact stiffness is being linearized as:

$$k_{hj} = c_H(u_w(t) - u_r(t) - \eta_r(t))_j^{1/2} \text{ if } u_{wj}(t) \geq u_{rj}(t) + \eta_{rj}(t)$$

$$k_{hj} = 0 \text{ if } u_{wj}(t) \leq u_{rj}(t) + \eta_{rj}(t) \quad (8)$$

$u_w(t)$  and  $u_r(t)$  are respectively the wheel and rail displacements,  $\eta_{rj}(t)$  the rail defects (irregularities, corrugation etc.) and  $c_H$  the Hertzian contact coefficient;  $k_{hj}$  and  $c_{hj}$  are respectively the Hertzian stiffness and damping contact coefficients.

### The track model

The railway track model is made up of the rail itself, rail pad which is represented as a massless series of spring and dampers inter connected to the sleepers assembled to ballast structure that is made up of granular concrete stones. The ballast is connected to the subgrade by a series of spring and dampers while this subgrade is directly linked to the natural soil. The spring-dampers systems couples together represent the viscos-elastic characteristics of the track components. The horizontal springs and dampers enables vibration transmission on the track structure with respect to the train sense of motion as seen in fig.1.

### Rail model

Since the railroad is considered as a continuous Timoshenko beam, in this work is used plane frame finite element discretized method to determine the vertical deflection. A finite length of the track is selected since the continuous beam can be divided into segments of sub beams elements.

### Railroad stiffness matrix

Considering the railroad as a uniform homogenous beam structure, the element stiffness matrix is written as  $K^e$  with a cross sectional moment of inertia  $I$ , rail cross sectional area  $A$ , the length of element ,  $L$  is the total length of the rail, material young modulus of elasticity  $E$ ,  $n_j$  nodes and

$n_{el}$  elements. The stiffness matrix is obtained in adding the axial and bending deformation sub matrices.

The analysis of a railroad can be undertaken by applying the stiffness matrix which is define as a series of beam elements ( $N_{el}$ ) connected to each other.

**Railroad mass matrix**

The lump mass method has been adopted because it takes in consideration the material properties of the rail. This method assumes that the mass coefficient of the beam correspond to its nodal coordinate and can be evaluated using the same procedure as that of the stiffness coefficients.  $L$  is the length of the  $i$ beam element illustrated in equation (8).

$$M_r^e = \int_0^L N(s)^T N(s) dv = \rho A \int_0^L N(s)^T N(s) dl \tag{8}$$

**Railroad damping matrix**

Since it is often difficult to use numerical solution to calculate the damping matrix of an element, but only the stiffness  $K$  and mass  $M$ , thus the damping matrix of the rail beam can be evaluated using the following Rayleigh damping theory (Ferrara R. and al., 2013):

$$[C^e] = \alpha [M^e] + \beta [K^e] \tag{9}$$

The realistic damping ratio of the  $n^{th}$  vibration mode of the rail system is obtained as

$$\zeta_n = \frac{\alpha}{2} \frac{1}{\omega_n} + \frac{\beta}{2} \omega_n \tag{10}$$

Where  $\alpha$  and  $\beta$  are constants to be determined from two given damping ratios  $\zeta_i$  and  $\zeta_j$  that correspond to two unequal frequencies of vibration  $\omega_i$  and  $\omega_j$  respectively. These two modes can be expressed in matrix form as:

$$\frac{1}{2} \begin{bmatrix} 1/\omega_i & 1/\omega_i \\ 1/\omega_j & 1/\omega_j \end{bmatrix} \begin{Bmatrix} \alpha \\ \beta \end{Bmatrix} = \begin{Bmatrix} \zeta_i \\ \zeta_j \end{Bmatrix} \tag{11}$$

The coefficient  $\alpha$  and  $\beta$  are determined in solving equation (11). (Ekevid and al., 2001) propose the following values  $\alpha = 0.005$  and  $\beta = 0.005$  for the calculation of the rail damping matrix.

**Equivalent nodal force of a rail element**

Considering geometrical feature of the car, it is possible to calculate the equivalent nodal force  $P_{ij}$ . To evaluate the load of the system  $F$ , the following terms are to be considered: the wheel-rail contact force  $P_0$ , the sleepers-rail contact forces  $P_{ij}''$  and the vertical distributed load of the rail  $q_0$ .

- The wheel-rail contact force in between two nodes is obtained from:

$$P_0 = N(s)^T * P_{w/r} \tag{12}$$

- The vertical force of a generic beam under uniformly distributed load is computed as:

$$F_0 = q_0 \int_0^L N(s)^T dl \tag{13}$$

- The sleepers-rail contact force can be evaluated when the connection force occurs either on the *i* or *j* rail connected to the sleepers as.

$$P_{ij}'' = \sum_{i=1}^n \frac{C_{rp}}{n} (\dot{U}_{r,i} - \dot{U}_{s,i}) + \sum_{i=1}^n \frac{K_{rp}}{n} (U_{r,i} - U_{s,i}) \tag{14}$$

In which *n* is the number of the rail paddampings and stiffnesses considered during simulation.

The material coefficient included in the above nodal force equation will be added in the damping and stiffness matrices of the rail and sleepers during the simulation process.

The rail general equation of motion in matrix form is:

$$[M_r]\{\ddot{u}_r\} + [C_r]\{\dot{u}_r\} + [K_r]\{u_r\} - [P_{c/r}] - [P_{sub/r}] = [-F_r(t)] \tag{15}$$

Where:  $[M_r]$ ,  $[C_r]$ ,  $[K_r]$ ,  $[P_{c/r}]$ ,  $[P_{sub/r}]$  and  $[-F_r]$  represent respectively overall mass, damping, stiffness, the equivalent vehicle-rail interaction force, substructure-rail equivalent force and lastly the equivalent nodal force matrices.

- **Rail-pad model**

The rail pad in presently work is modeled as a contact area, which is assumed as viscous layer distributed in between the rail foot and the sleepers. The total stiffness and damping are obtained as, with *n* representing the number of stiffness and damping coefficient that constitutes the rail-pad.

$$\text{stiffness: } K_{rp} = \sum_{i=1}^n \frac{k_{rp}}{n} \text{ and damping: } C_{rp} = \sum_{i=1}^n \frac{c_{rp}}{n}$$

- **Sleeper model**

The dynamic equation of motion for the *m<sup>th</sup>* sleeper is evaluated as:

$$m_{si}\ddot{u}_{si}(t) + (C_{bi} + C_{rpi})\dot{u}_{si}(t) - C_{bi}\dot{u}_{bi}(t) - C_{rpi}\dot{u}_r(t) + (K_{bi} + K_{rpi})u_{si}(t) - K_{bi}u_{bi}(t) - K_{rpi}u_r(t) = f_s(t) \tag{16}$$

- **Ballast model**

The continuous granular ballast is modeled as a series of separate vibrating masses, by which the analytical process of the ballast vibration is greatly simplified. The method used to determine ballast vibration is in accordance with(Zhai and al.,2004).

The vibrating mass and stiffness of the ballast under a sleeper supported are determined from:

$$M_b = \rho_b h_b (l_e l_1 + (l_e + l_b) h_b \tan \alpha + \frac{4}{3} h_b^2 \tan^2 \alpha) \quad (17)$$

$$k_b = \frac{2(l_e - l_b) \tan \alpha}{\ln[(l_e / l_b) \cdot (l_b + 2h_b \tan \alpha) / (l_e + 2h_b \tan \alpha)]} E_b \quad (18)$$

The ballast damping coefficient  $C_b$  is obtained using the curve fitting theory while the coefficients for longitudinal springs and dampers are obtained according to the theory of (Sun and Dhanasekar, 2002).

$$K_{bo_i} = \frac{30}{100} K_{b_i} \text{ and } C_{bo_i} = \frac{30}{100} C_{b_i} \quad (19)$$

- the equation of motion of the  $m^{th}$  ballast block

$$m_{b_i} \ddot{u}_{b_i}(t) + (2C_{bo_i} + C_{b_i} + C_{sg_i}) \dot{u}_{b_i}(t) + (2K_{bo_i} + K_{b_i} + K_{sg_i}) u_{b_i}(t) - C_{bo_i} \dot{u}_{b_{i+1}}(t) + C_{bo_i} \dot{u}_{b_{i-1}}(t) - K_{bo_i} u_{b_{i+1}}(t) - K_{bo_i} u_{b_{i-1}}(t) - C_{b_i} \dot{u}_{s_i}(t) - K_{b_i} u_{s_i}(t) = f_{b_i}(t) \quad (20)$$

• **Subgrade model**

The modulus of subgrade stiffness under supporting point is determined as:

$$K_f = (l_b + 2h_b \tan \alpha)(l_e + 2h_b \tan \alpha) \rho_b \quad (21)$$

Here  $\rho_b, h_b$  are the density, the depth of the ballast respectively,  $\alpha$  is the ballast stress distribution angle,  $l_e$  the effective supporting length of the half sleepers and  $l_b$  the width of the sleeper's underside.

The general equation of motion for the track structure:

$$[M_T] \{\ddot{u}_T\} + [C_T] \{\dot{u}_T\} + [K_T] \{u_T\} - [P_{C/T}] = [F_T] \quad (22)$$

In which  $[M_T], [C_T], [K_T], [P_{C/T}]$  and  $[F_T]$  are the generalized mass, damping, stiffness, wheel-rail contact force and force of the track components matrices respectively.

**Methods of resolution**

Today, the finite element method is considered as one of the well established and convenient technique for computer solution of complex problems such as that of the train and track structure. As a complex system the train - track dynamic equations of motion are modeled and summarized according to equations (6) for the vehicle and (22) for the track.

**System discretization**

The systems of equations (6) and (22) will be resolved using the classical Newmark method. It is a scheme that permits the evaluation of solutions with respect to time interval  $[t_n, t_{n+1}]$  variation. Known as a linear acceleration method, displacement and velocity are written in function of acceleration respectively.

$\Delta t = t_{n+1} - t_n$  and  $u_{n+1}, \dot{u}_{n+1}, \ddot{u}_{n+1}$  verify the systems of following equations:

$$u_{n+1} = u(t_{n+1}) \approx u_n + \Delta t \dot{u}_n + (1 - \beta_2) \frac{\Delta t^2}{2} \ddot{u}_n + \frac{\beta_2 \Delta t^2}{2} \ddot{u}_{n+1} \quad (23)$$

$$\dot{u}_{n+1} = \dot{u}(t_{n+1}) \approx \dot{u}_n + (1 - \beta_1) \Delta t \ddot{u}_n + \beta_1 \Delta t \ddot{u}_{n+1} \quad (24)$$

Where  $\beta_1$  and  $\beta_2$  are integration coefficients.

Replacing equations (23) and (24) in (6) and (22), thus:

$$F_{c(n+1)}(\ddot{u}_{c(n+1)}) = A_c \ddot{u}_{c(n+1)} - P_{c(n+1)}(\ddot{u}_{c(n+1)}) + B_{c,i} \quad (25)$$

$$F_{T(n+1)}(\ddot{u}_{T(n+1)}) = A_T \ddot{u}_{T(n+1)} - P_{T(n+1)}(\ddot{u}_{T(n+1)}) + B_{T,i} \quad (26)$$

Where:  $A_c = \left[ M_c + C_c \beta_1 + K_c \beta_2 \frac{\Delta t^2}{2} \right]$  and  $A_T = \left[ M_T + C_T \beta_1 + K_T \beta_2 \frac{\Delta t^2}{2} \right]$

$$B_{c,i} = \left\{ C_c \left[ \dot{u}_{c(n)} + (1 - \beta_1) \Delta t \ddot{u}_n + \right. \right. \\ \left. \left. + K_c \left[ u_{c(n)} + \Delta t \dot{u}_n + (1 - \beta_2) \frac{\Delta t^2}{2} \ddot{u}_n \right] \right\}$$

$$B_{T,i} = \left\{ C_T \left[ \dot{u}_{T(n)} + (1 - \beta_1) \Delta t \ddot{u}_n + \right. \right. \\ \left. \left. + K_T \left[ u_{T(n)} + \Delta t \dot{u}_n + (1 - \beta_2) \frac{\Delta t^2}{2} \ddot{u}_n \right] \right\}$$

### Numerical resolution

The wheel-rail contact model presents the phenomenon of non-linearity in the system of equations above (25-26). So, Newton Raphson iterative method has been adopted in resolution. At the initial state where the iterative  $k = 0$ , the  $(n+1)$  solution of the displacement that corresponds to speed and acceleration are denoted as:

$$u_{n+1}^0 = u_n \quad \dot{u}_{n+1}^0 = \dot{u}_n \left( 1 - \frac{2\beta_1}{\beta_2} \right) + \ddot{u}_n \left( 1 - \frac{\beta_1}{\beta_2} \right) \Delta t \quad \ddot{u}_{n+1}^0 = \\ \dot{u}_n \frac{2}{\Delta t \beta_2} + \ddot{u}_n \left( 1 - \frac{1}{\beta_2} \right) \quad (27)$$

### Construction of the R matrix

The P matrix constitutes the derivatives of all the wheel-rail contact forces. For proper construction of this matrix, it should be noted that  $R_{11}$  and  $R_{12}$  are related to the equation of the vehicle (wheels) and also contain the derivative of the wheel-rail contact forces with respect to the wheel acceleration while  $R_{21}$  and  $R_{22}$  correspond to that of the track and contain the derivative of the wheel-rail contact forces with respect to the rail nodes as in equation (7). So R matrix and its components can be evaluated as:

$$R_{n+1}^k = \begin{bmatrix} R_{11(n+1)}^k & R_{12(n+1)}^k \\ R_{21(n+1)}^k & R_{22(n+1)}^k \end{bmatrix} \tag{28}$$

After obtaining the Jacobian J of the above equations system (25-26), the solution of the acceleration can then be calculated as:

$$J(\ddot{u}_{n+1}^k)(\ddot{u}_{n+1}^{k+1} - \ddot{u}_{n+1}^k) = -F(\ddot{u}_{n+1}^k) \tag{29}$$

where  $k$  is the Newton Raphson iteration and  $n$  is the time to time step during simulation.

The train and the track parameters used for the simulation of our model are structured in the 1 and 2tables:

Table 1: Locomotive CC2600 parameters (Lezin and *al.*, 2012).

Notation	Parameters	Values	Units
$2M_7$	Car body mass	18.8	<i>ton</i>
$M_{BG}$	Bogie mass	3000	<i>kg</i>
$M_w$	Wheel mass	5500	<i>kg</i>
$L_7$	Length of train	23.54	<i>m</i>
$L_w$	Length of wheel base	2.5	<i>m</i>
$L_{BG}$	Length of bogie bases	17	<i>m</i>
$K_0$	Primary suspension stiffness	$86.10^4$	<i>N/m</i>
$C_0$	Primary suspension damping	$3.10^3$	<i>Ns/m</i>
$K_6$	secondary suspension stiffness	$12.10^6$	<i>N/m</i>
$C_6$	secondary suspension damping	$15.10^3$	<i>Ns/m</i>

## Result and discussion

The simulating results using MATLAB are presented in two phases. Firstly the behavior of the vehicle and steady state response of the track components in the time domain are presented. Next the vibration mode of the vehicle and the track components are evaluated in which the displacement, velocity, acceleration and the effect of the dynamic load on the rail are illustrated.

### Behavior of the vehicle

At  $t = 0.34s$ , the car body displacement  $u_7 = 0.023m$ , At  $t = 0.32s$ , the displacement of the bogie  $u_{5,6} = 0.0087m$  while at  $t = 0.22s$ ,  $u_{wj} = 0.01004m$ . It is notice that  $u_{5,6} < u_{wj} < u_7$  which is due to the effect of the primary and secondary suspension parameters, and the non linearity that exist in between the wheel and the rail contact surfaces.

Table 2: Track parameters (Lezin and *al.*, 2012) and (De Man, 2000)

Notation	Parameters	Values (per rail seat)	Units
EI	Rigidity modulus	4.47	MN. m <sup>2</sup>
I	Inertia moment	2127	cm <sup>4</sup>
A	Rail cross section area	69.34. 10 <sup>-4</sup>	m <sup>2</sup>
m <sub>r</sub>	Mass of the rail (per unit length)	54	kg/m
m <sub>s</sub>	Sleeper mass (half)	125,5	kg
l <sub>s</sub>	Sleepers spacing	60	cm
l <sub>e</sub>	Effective support length of half sleeper	0,95	m
l <sub>ws</sub>	Sleeper width	0,30	m
m <sub>b</sub>	Ballast mass	700	kg
h <sub>b</sub>	Ballast thickness	0.45	m
α <sub>b</sub>	Ballast stress distribution angle	35	°
k <sub>rp</sub>	Rail pad stiffness	11,92.10 <sup>8</sup>	N/m
c <sub>rp</sub>	Rail pad damping	29,28.10 <sup>3</sup>	Ns/m
k <sub>b</sub>	Ballast vertical stiffness	24.10 <sup>7</sup>	N/m
c <sub>b</sub>	Ballast vertical damping	58,8.10 <sup>3</sup>	Ns/m
k <sub>b0</sub>	Ballast horizontal stiffness	7,2.10 <sup>7</sup>	N/m
c <sub>b0</sub>	Ballast horizontal damping	17,64.10 <sup>3</sup>	Ns/m
E <sub>SG</sub>	Subgrade K <sub>30</sub>	9.10 <sup>7</sup>	Pa/m
k <sub>SG</sub>	Subgrade stiffness	7,68.10 <sup>7</sup>	N/m
c <sub>SG</sub>	Subgrade damping	64,6.10 <sup>3</sup>	Ns/m

Fig. 2 is illustrative of the car body, bogie and wheel vertical displacements. And Figs. 3 show the vertical displacement acceleration of the bogie and the wheels, so at t = 0.01 s, the maximum acceleration of the bogie is  $\ddot{u}_{5,6} = 0.00091 \text{ m/s}^2$ . It rapidly decelerates to  $\ddot{u}_{5,6} = -0.00045 \text{ m/s}^2$  at t = 0.29s and regains its stability when  $\ddot{u}_{5,6} = -0.00088 \text{ m/s}^2$  at time step t = 1.35s. At t = 0.2 s, the maximum vertical displacement velocity of rail is  $\dot{u}_r = 70 \text{ mm/ms}$  and has as minimum  $\dot{u}_r = -0.012 \text{ mm/ms}$  and regains stability at t = 0.3 s (see Fig. 4).

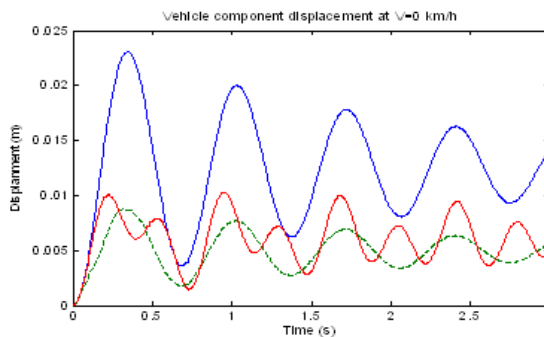


Fig. 2: Comparison of the car body, bogie and wheel displacement

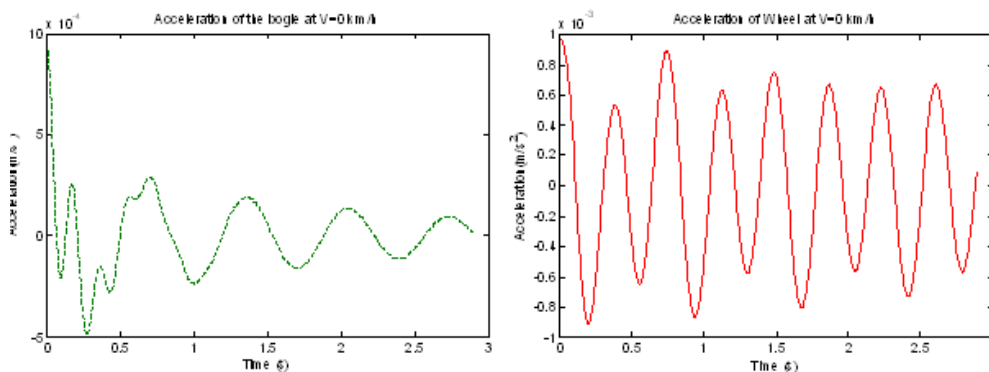


Fig. 3: Bogie and wheel acceleration at  $v = 0 \text{ km/h}$

At time step  $t = 0.0\text{s}$ , the maximum static load of the locomotive on the rail is 110 kN. At time step  $t = 0.05\text{s}$ , the load increases on the rail and becomes almost 135 kN (fig. 4 below) while minimum load is 20 KN. This shows the behavior of the vehicle dynamic load on the rail during starting. If this load is above the maximum value that track components can support, deformations will occur either on the wheel or on the track components (principally the rail). All those troubleshootings and phenomena of fatigue will induce failures on the locomotive or the railway track components.

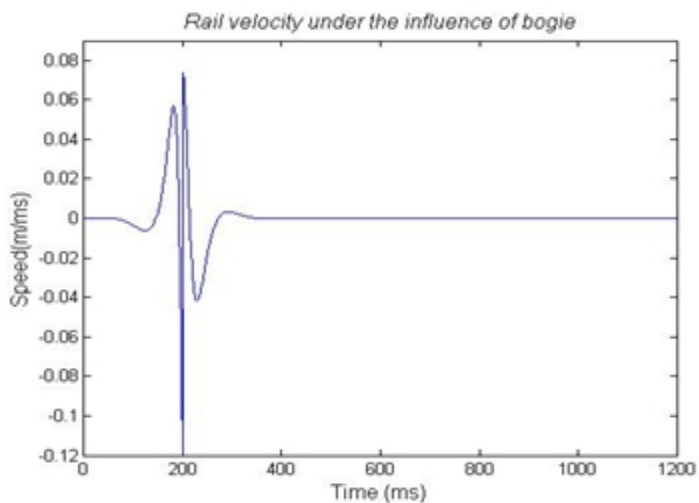


Fig. 4: Rail velocity under the influence of bogie

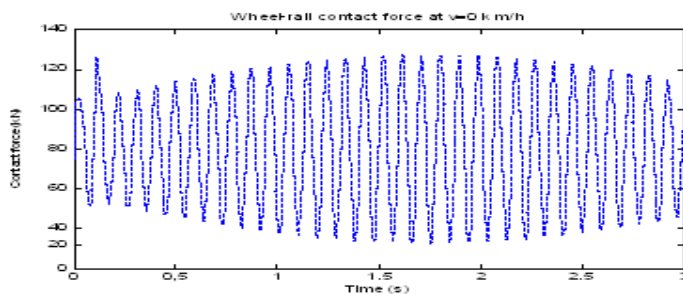


Fig. 5: Effect of load on the rail during starting and steady state response.

According to numerical simulation, the displacements of each track components under steady state response are presented.

Fig. 5 is illustrative of the time history of the load on the rail under excitation of the vehicle. At  $t = 0$  the applied load on the track is static and the rail resists to displacement until  $t = 0.081s$  when deflection starts. The rail deflection maximum of 2.805 mm occurs at time  $t = 0.192 s$ . Furtherly it repeats itself at  $t = 0.213s$ . However at  $t = 0.2 s$  the displacement becomes smaller 1.5 mm, this explains the behavior of the rail under constant excitation.

The time history of sleeper vertical displacement illustrates that at  $t = 0$  the sleeper resist ~~on~~ displacement until  $t = 0.081s$  where displacement starts and becomes maximum at  $t = 0.19s$  i.e. 1.606 mm, furtherly repeats itself at  $t = 0.214s$ . At  $t = 0.2s$  the displacement is 0.98 mm.

The time history for ballast vertical displacement at  $t = 0$  the load is fixed on the rail and the ballast resist deflection until  $t = 0.081s$ , it starts and becomes maximum at  $t = 0.19 s$  i.e.  $u_b = 0.791 mm$ , repeats itself at  $t = 0.214s$ . At  $t = 0.2s$  the displacement is  $u_b = 0.405 mm$ .

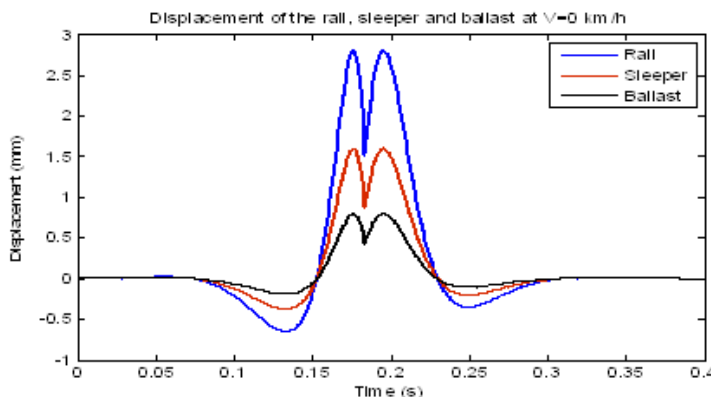


Fig. 5: Time history displacement of track components under steady state response.

From fig. 4, it is seen that the peak of the rail vertical velocities is between  $-0.012$  mm/s and  $0.07$  mm/s while that of accelerations lies between  $0.529$  m/s<sup>2</sup> and  $0.85$  m/s<sup>2</sup>. They occur in correspondence of the four wheel-set effect on the rail and also show the effect of nonlinearity that exists in between the rail and the wheel contact. These values vary as the load from the train increases.

The acceleration of the sleepers(fig.6) under steady state effect of the locomotive lies between  $0.026$  m/s and  $0.028$ m/s and  $0.82$  m/s<sup>2</sup> and  $1.64$  m/s<sup>2</sup> respectively.

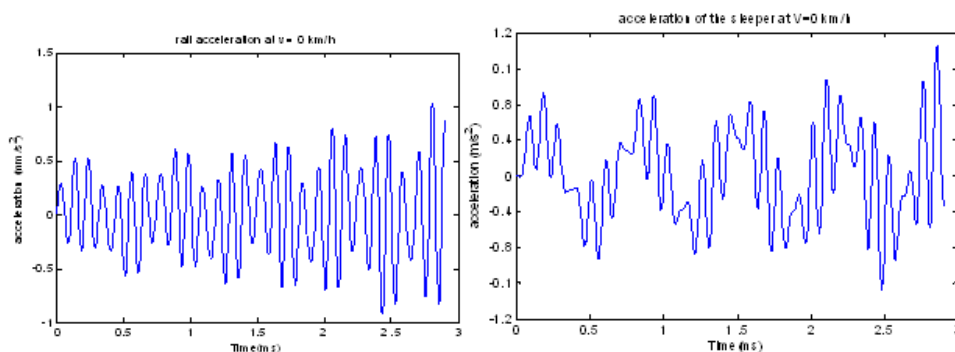


Fig. 6: Rail and sleeper acceleration at  $v = 0$  km/h

## Conclusion and perspectives

The dynamic model has been developed to predict train-track vibration. The Discret Element Method (DEM) has been used to model the vehicle while the rail is modeled using finite elements method. A mathematical model that explains the dynamic behavior of the system has been developed. Newmark time discretization and Newton Raphson iteration methods are used to resolve dynamics equations in MATLAB. The vehicle is considered as a harmonic load vertically applied on the track structure and the dynamic effects of the train track components are studied during starting and steady state response. Load evaluation on rail, deflection, velocity and acceleration had been calculated for each time step. The rail presents maximum effects in the analysis as compare to sleepers and the ballast embankment.

It can be concluded that when vertical displacements of the rail, sleeper and ballast are more than their maximum values, deformation occur and create rail irregularities, corrugation, bad geometry and heterogeneities of the ballast materials. These phenomena increase vibration mode on the track structure and train induces vibrations that affect the ride comforts and arriving time of goods and passengers. The parameters of the vehicle

components need to be taken into consideration because the influence vibrations behaviour of the track will affect the cost of maintenance and operating time of the railway line.

As future works, the following need to be done:

- Develop a package for the simulation of train-track system which will take in consideration the following phenomenon: rail irregularities and corrugations.
- Study the behavior of the track components under the lateral displacements relative to the vertical one of the train.
- Carry out experimental analysis at Camrail (transcam 2 and 3) so as to validate analytical and numerical results.
- Integrate the domain of maintenance at the level of train track design.

### References:

Collette C., Mihaita H. and Andre P., (2008). Rotational vibration absorber for the mitigation of rail rutting corrugation, *Vehicle System Dynamics*, Vol. 00, No. 0, 1–19

De Man A. P. (2000). Pin-pin resonance as reference in determining ballasted rail track vibration behaviour. *Delft University of Technology, Faculty of Civil Engineering and Geosciences, Railway Engineering Group*, P.O. Box 5048, NL-2600 GA Delft.

Dumitriu M. (2012). Influence of the suspension system on the ride comfort of the passenger ride comfort of passenger railway vehicle, *U.P.B., SCI, Bull, Serie D*, vol 74, ISS, 16.

Ekevid T., Li M. X. D. and Wiberg N. E. (2001). Adaptive FEA of wave propagation induced by high-speed trains, *Computers and Structures*, 79, 2693-2703.

Fermér M. and Jens C.O. Nielsen, (1995). Vertical interaction between train and track with soft and stiff rail pads, *full-scale experiments and theory*. Volume 209, pages 39 – 47.

Ferrara R., Leonardi G., and Jourdan F., (2013). Numerical modelling of train induced vibrations. *Procedia - Social and Behavioral Sciences*, 53(0):155 – 165, ISSN

Graissie S.L., Gregory R. W., Johnson K.L., (1982). The dynamic response of railway track to high frequency longitudinal excitation. *Journal of mechanics and engineering science*.24 (2), 97-102.

Hai Huang and Steven Chrismer, (2013). Discrete element modeling of ballast settlement under trains moving at critical speeds, *Construction and Building Materials*, 38(0):994 – 1000, ISSN 0950-0618

Huan Feng, (2011). 3d-models of railway track for dynamic analysis, PhD thesis in mechanical engineering. *Department of transport science, school of*

*architecture and the built environment, royal institute of technology Stockholm.*

Jabbar A. Z., He Xie and Jun J.F., (2009).Dynamic response of train-track system to single rail irregularity. *Latin American journal of solid and structure*, 6, 89-104

Knothe KL. and Grassie S.L., (1993).Modeling of railway track and vehicle/track interaction at high frequencies.*Vehicle System Dynamics*, 22(3-4):209–262.

Lezin Seba Minsili, Madja Doumbaye Jeremie, Grace L. Tsebo Simo and Christiane Simo (2012). Preventive maintenance of railway tracks: Ballast performance anticipation in the Cameroon railway. *Research journal of applied science, engineering and technology* 4(5): 398-406.

Mazilu T., (2007). Wheel/rail interaction due to parametric excitation. *U.P.B. Scientific bulletin series D, Mechanical engineering*, Vol. 69, 16 pages.

Oliveira M. H. Z., Rocha S. S., Barbosa F. S. and Nogueira F. M. A., (2010). Numerical and experimental analysis of the train-railway interaction. *Universidade Federal de Juiz de Fora, Juiz de Fora, Brazil*, 09 pages.

Robert and Czeslaw, (2000). Experimental analysis of railway track vibration on straight and curve sections, *Journal of sound vibration*, V. 21. 467-477.

Sato Y., (1977).Study on high-frequency vibration in track operated with high speed train. *JNR. Qua*, 18 (3): 109-114.

Sun Y.Q. and Dhanasekar M., (2002). A dynamic model for the vertical interaction of the rail track and wagon system. *International Journal of Solids and Structures*, 39(5):1337 – 1359.

Yang H., Wang K. and Cheng H., (2012).Characteristics of wheel-rail vibration of vertical section of high speed train. *Journal of modern transport*, V.20, 10-15.

Zhai W.M., Wang K.Y., and Lin J.H., (2004). Modelling and experiment of railway ballast vibrations. *Journal of Sound and Vibration*, 270(4-5):673 – 683.

Zhang J., Gao Q., Tan S.J., and Zhong W.X., (2012). A precise integration method for solving coupled vehicle track dynamics with nonlinear wheel rail contact. *Journal of Sound and Vibration*, 331(21):4763 – 4773.

Zurich, (1926) Method of analysis of statical and dynamical stress in rails. 2nd Int. Congress of Applied Mechanics. 407-418.